BACT-3D: A LEVEL SET SEGMENTATION APPROACH FOR DENSE MULTI-LAYERED 3D BACTERIAL BIOFILMS

Wang, J., R. Sarkar, A. Aziz, A. Vaccari, A. Gahlmann, S.T. Acton

ICIP • Beijing
Sep. 20th, 2017

Overview

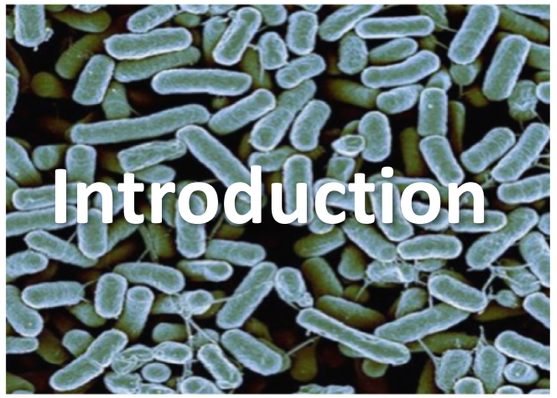
Introduction

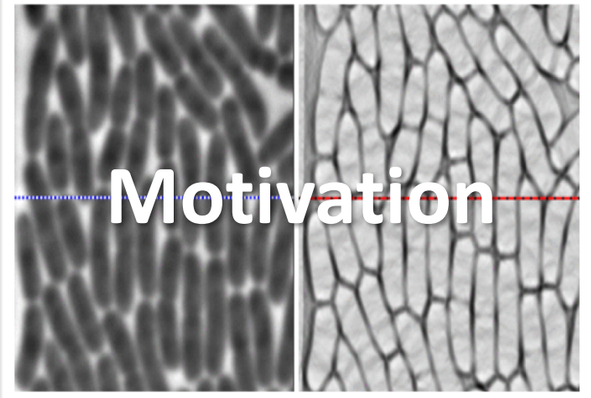
Motivation

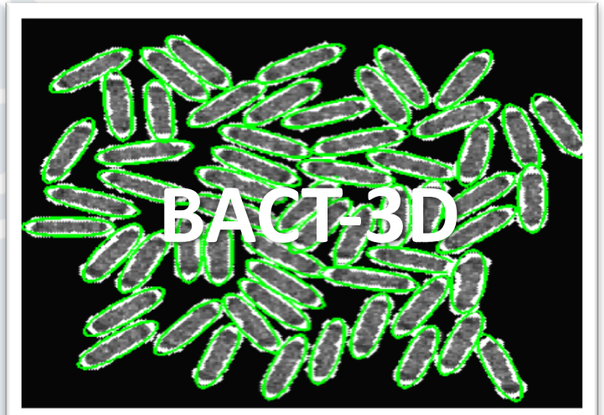
BACT-3D

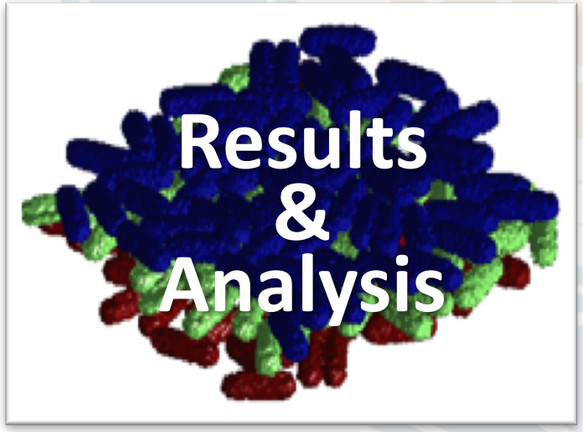
Results
&
Analysis

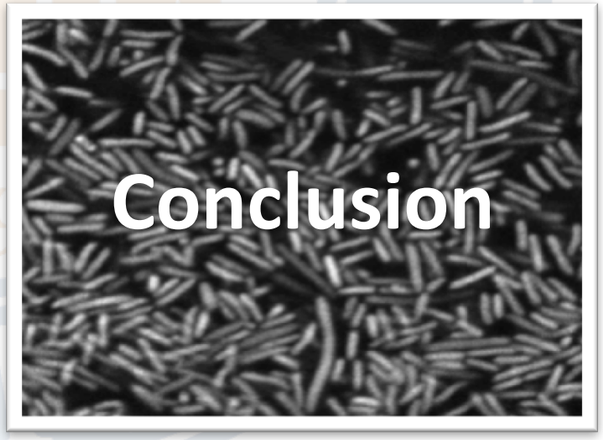
Conclusion

Introduction

[1]

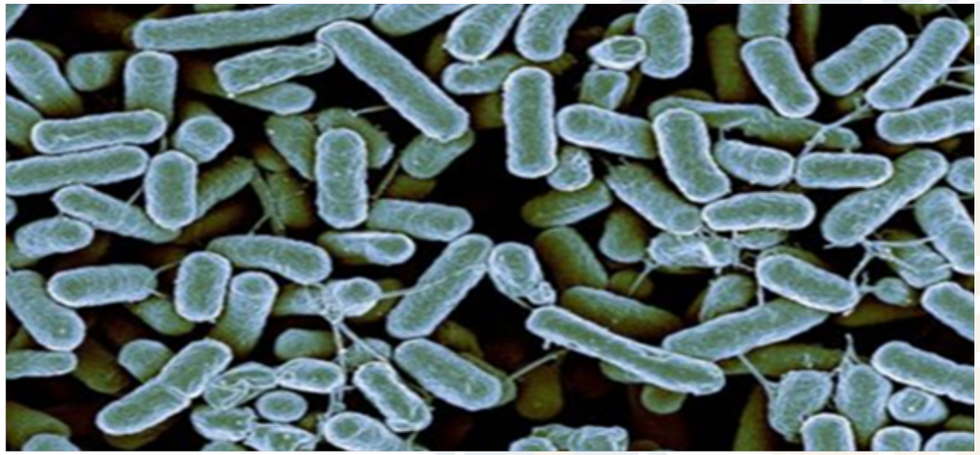

[2]

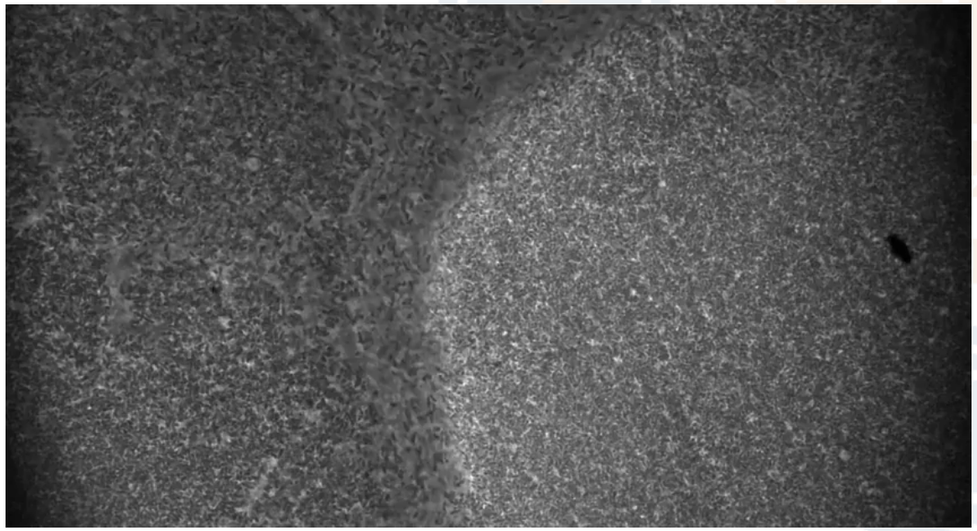

- Live in dense aggregations: Biofilms
  - Cellular contacts;
  - Essential ecological processes;
  - High antibiotic resistance.

- Shewanella oneidensis MR-1 biofilms, Gahlmann Lab, UVa.
  - Limited understanding of individual bacteria in crowed environment.

[1]: Peter Raven, Kenneth Mason, Jonathan Losos, and Susan Singer, “https://commons.wikimedia.org/w/index.php?curid=44194140,” Biology 10e Textbook.
[2]: https://youtu.be/6Cx62zS0Yp0

- **Super-resolution Imaging Technique**

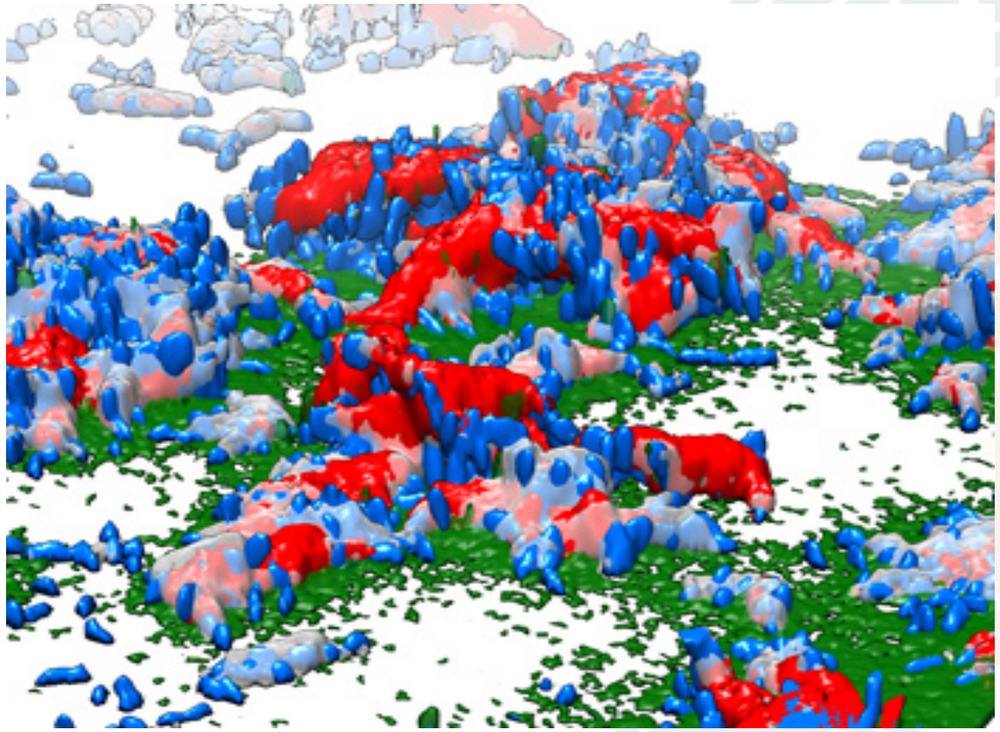

[1]

Traditional optical confocal microscopy

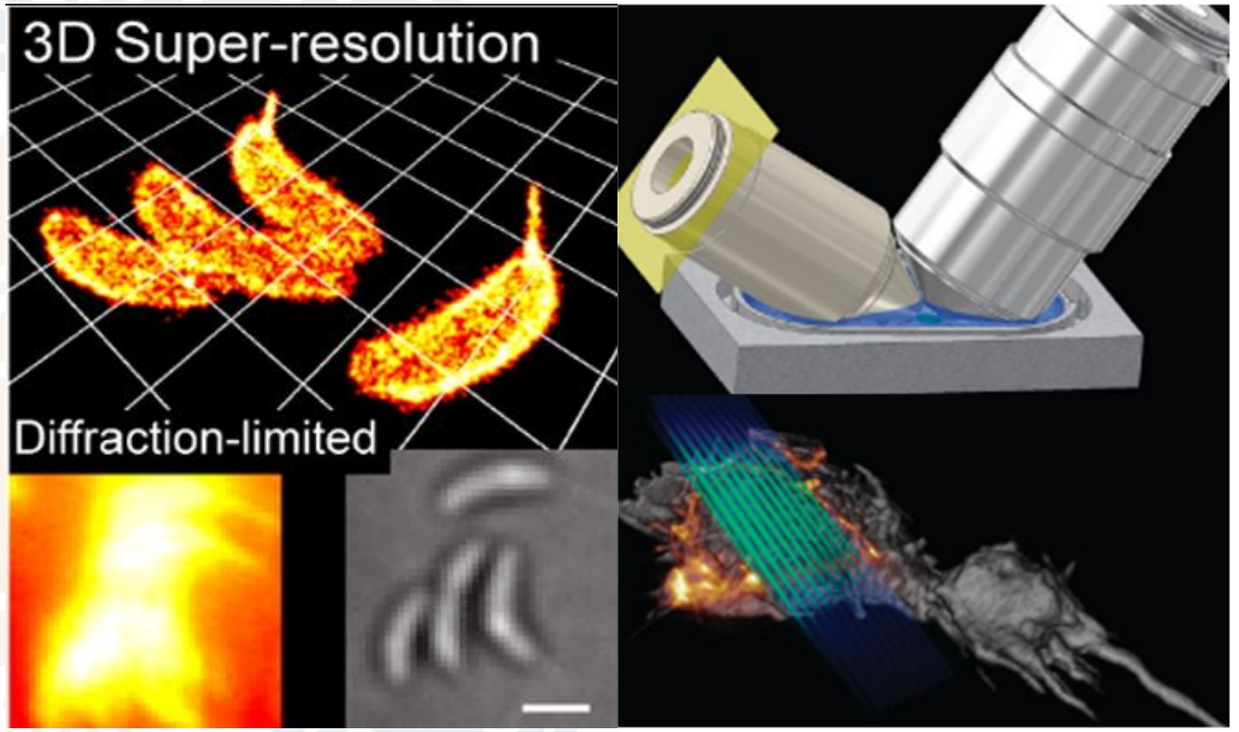

[2]

Super-resolution microscopy

[1]: Veysel Berk, Jiunn C. N. Fong, Graham T. Dempsey, et al., “Molecular architecture and assembly principles of vibrio cholerae biofilms,” Science, vol. 337, pp. 236–239, 2012.
[2]: Marissa K. Lee, Prabin Rai, Jarrod Williams, et al., “Small-molecule labeling of live cell surfaces for three-dimensional superresolution microscopy,” Journal of the American Chemical Society, vol. 136, pp. 14003,àí14006, 2014.

Previous Segmentation Methods

- **Edge Detection [1]:**
  Affected by image noise.

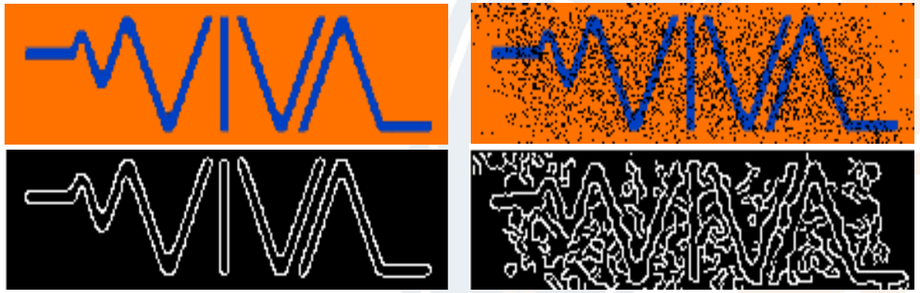

- **Vector Field Convolution [3]:**
  Special initialization required.

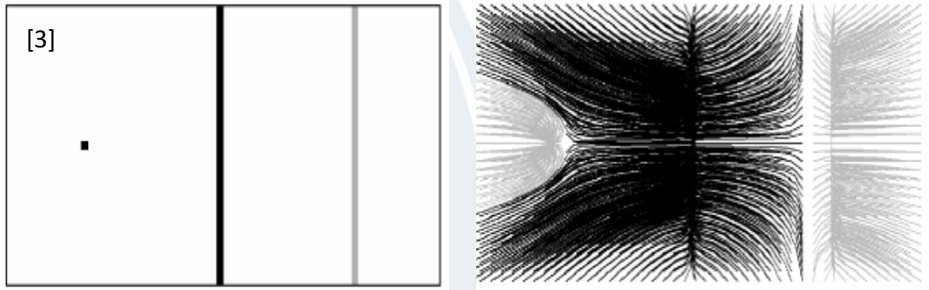

- **Watershed [2]:**
  Sensitive to intensity changes.

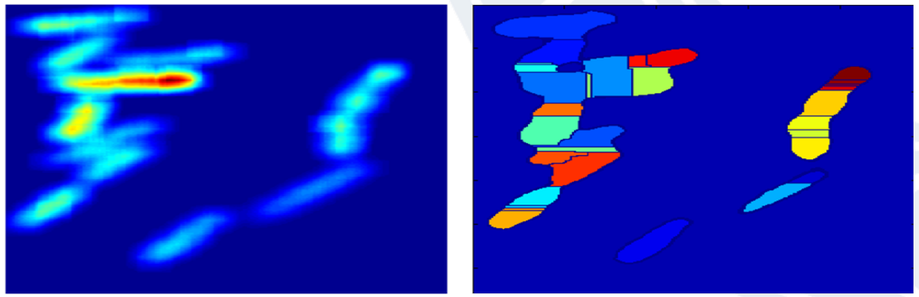

- **Seeded Watershed[4]:**
  Challenges in dense-community performance.

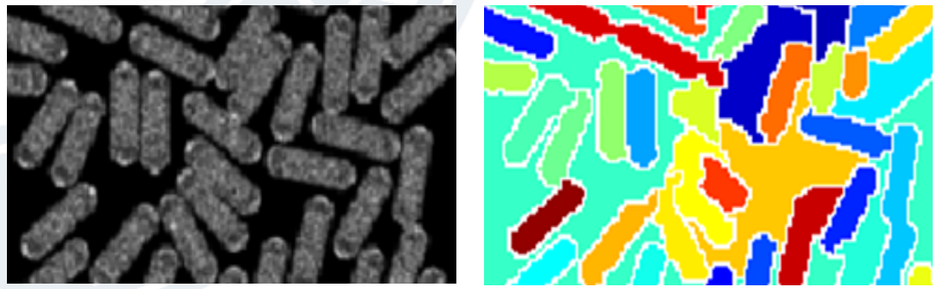

[1] T. Lindeberg and M. Li, “Segmentation and classification of edges using minimum description length approximation and complementary junction cues,” CVIU, 67(1), pp. 88–89, 1997.
[2]: L. Vincent and P. Soille, “Watersheds in digital spaces: an efficient algorithm based on immersion simulations,” IEEE Transactions on Pattern Analysis and Machine Intelligence, vol. 13, no. 6, pp. 583–598, 1991.
[3]: Bing Li and Scott T. Acton, “Active contour external force using vector field convolution for image segmentation,” IEEE Transactions on Image Processing, vol. 16, no. 8, pp. 2096–2106, 2007.
[4]: Pinidiyaarachchi, Amalka, and Carolina Wählby. "Seeded watersheds for combined segmentation and tracking of cells." *Image Analysis and Processing–ICIAP 2005* (2005): 336-343.

- **Chan Vese [1]:**

  Define the image into foreground and background.

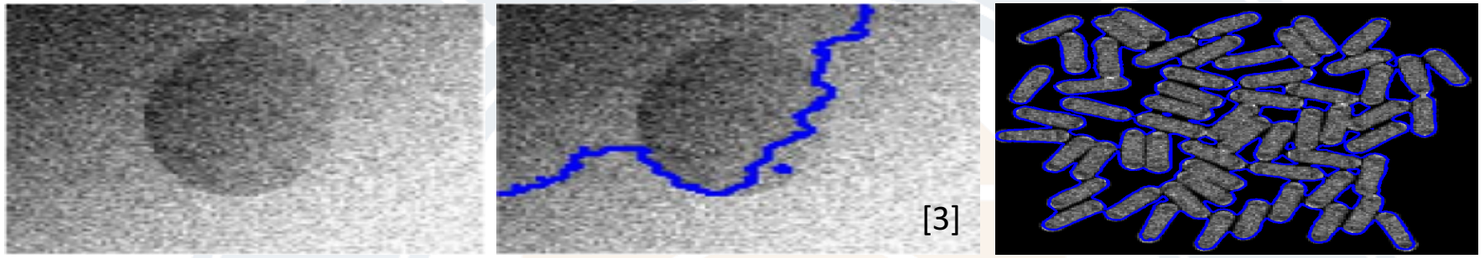

- **L2S [2]:**

  Model the inhomogeneity in the images as linear combination of Legendre polynomials.

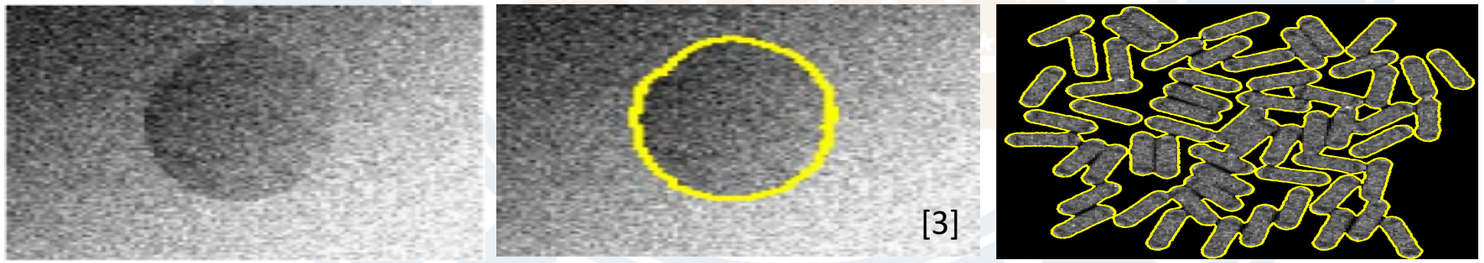

[1]: T. F. Chan and L. A. Vese, “Active contours without edges,” IEEE Transaction of Image processing, vol. 10, no. 2, pp. 266–277, 2001.
[2]: S. Mukherjee and S. T. Acton, “Region based segmentation in presence of intensity inhomogeneity using Legendre polynomials,” IEEE SPL, vol. 22, no. 3, pp. 298–302, March 2015.
[3]: Three images idemonstrate the failure of Chan Vese in noisy environment are from L2S.

- # Cell splitting methods

Splitting touching cells based on concave points [1]:

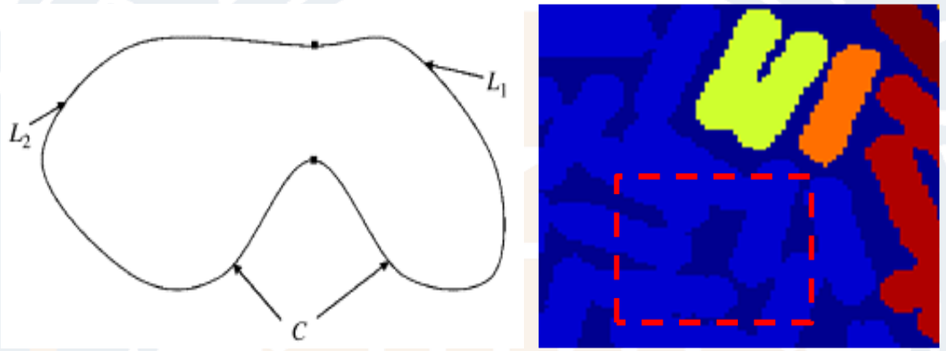

Splitting touching cells based on gradient flow [2]:

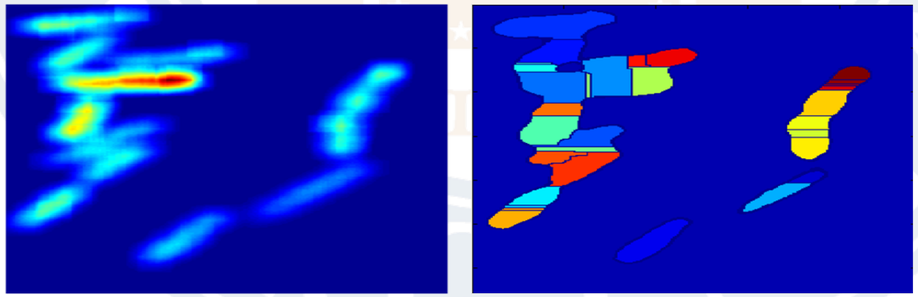

[1] X. Bai, C. Sun, and F. Zhou, “Splitting touching cells based on concave points and ellipse fitting,” Pattern Recognition, vol. 42, pp. 2434,Äì2446, 2009.
[2] L. Vincent and P. Soille, “Watersheds in digital spaces: an efficient algorithm based on immersion simulations,” IEEE Transactions on Pattern Analysis and Machine Intelligence, vol. 13, no. 6, pp. 583–598, 1991.

• Other integrated methods

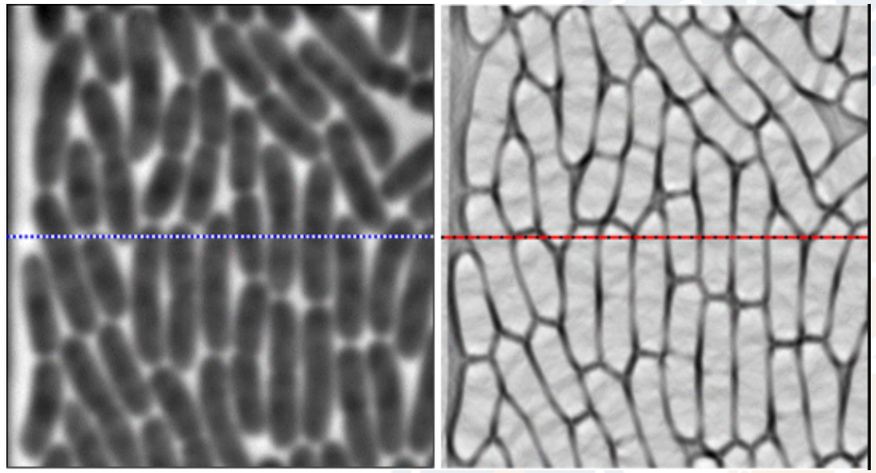

- S. K. Sadanandan, ¨O. Baltekin, K. E. G. Magnusson, et al., "Segmentation and track-analysis in time-lapse imaging of bacteria," IEEE Journal of Selected Topics in Signal Processing, vol. 10, no. 1, pp. 174–184, 2016.

$$weight = 0.5 \times RAR + 0.5 \times convexity$$

$$RAR = \frac{\min(area_{object}, ellipsearea)}{\max(area_{object}, ellipsearea)}$$

$$convexity = \frac{area_{object}}{area_{convexhullofobject}}$$

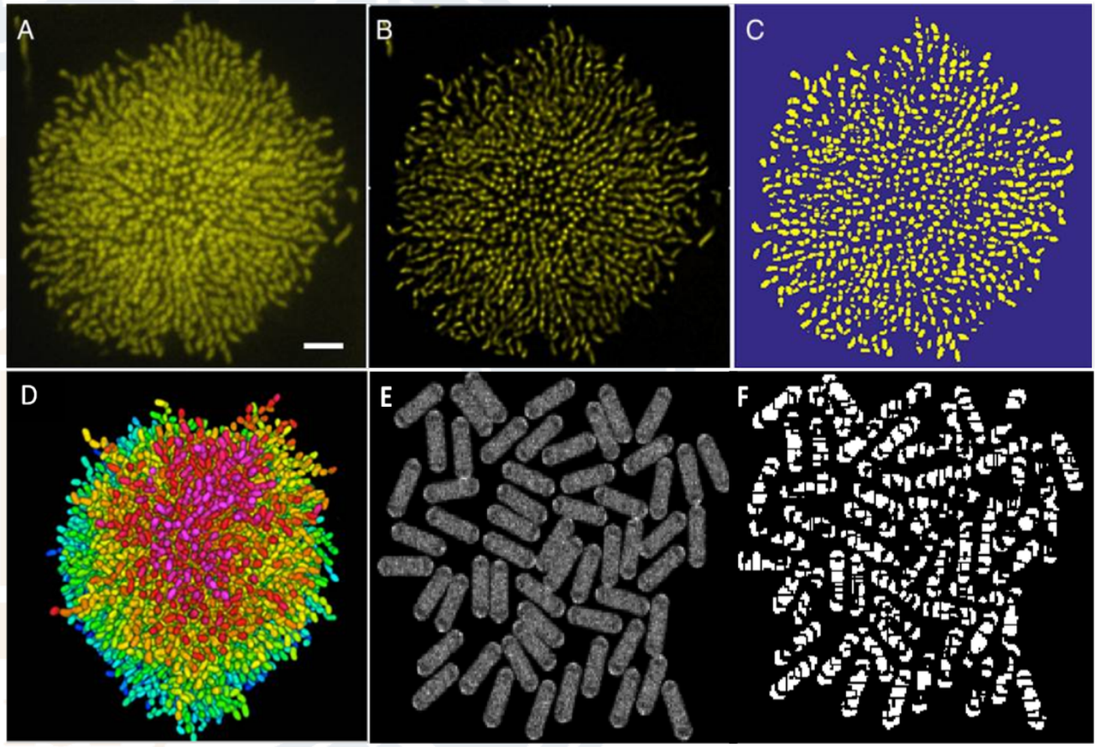

- J. Yan, A.G. Sharo, H. A. Stone, N. S. Wingreen, and B. L. Bassler, "Vibrio cholerae biofilm growth program and architecture revealed by single-cell live imaging," Proceedings of the National Academy of Sciences, vol. 113, no. 36, pp. E5337–E5343, 2016.

A. Raw data → B. Deconvolved image
→ C. Projection (Watershed) → D. Reconstruction

Bact-3D

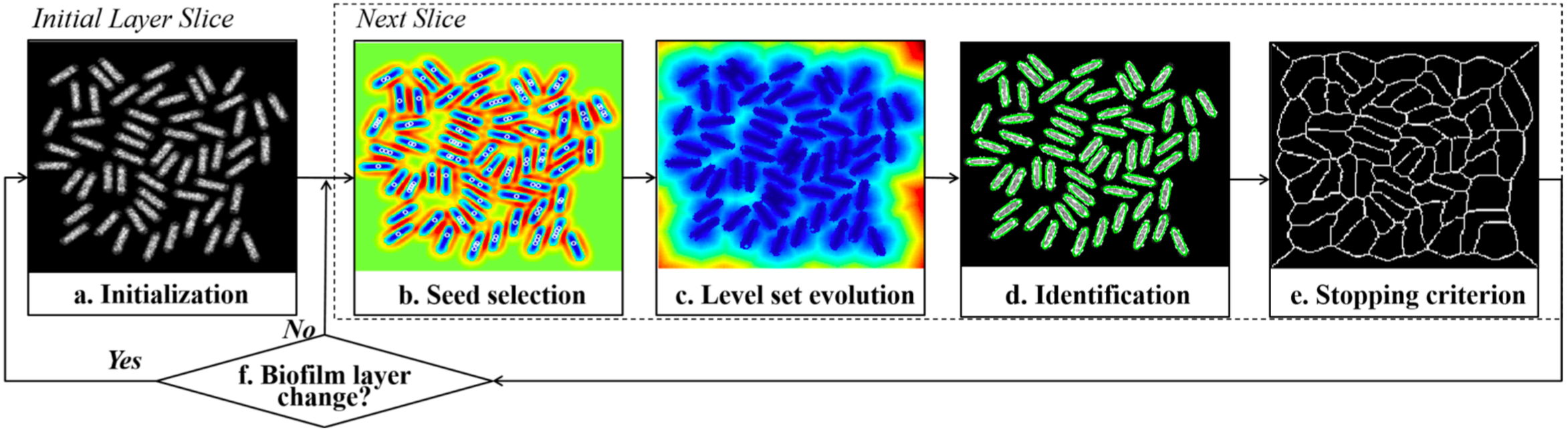
Initial Layer Slice
Next Slice
a. Initialization
b. Seed selection
c. Level set evolution
d. Identification
e. Stopping criterion
No
Yes
f. Biofilm layer change?

• Dataset generation

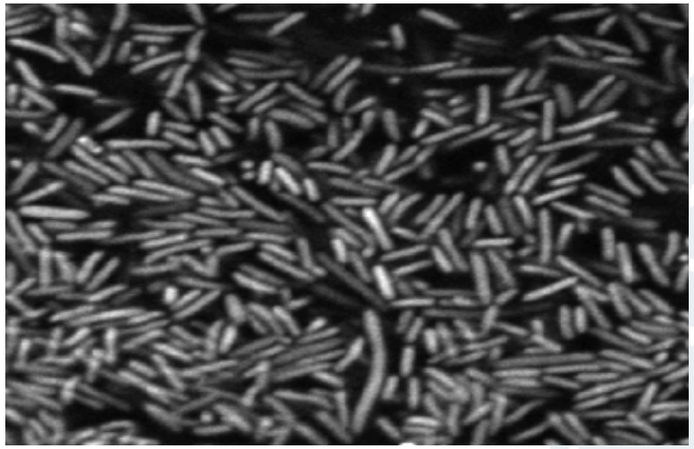

A. Multi-layered dense biofilms

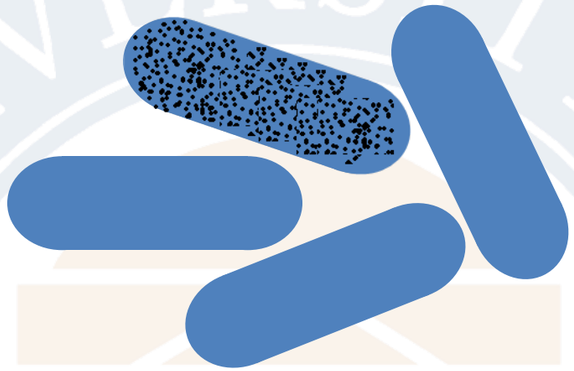

B. Construct bacterial structure
C. Simulate fluorescence emission

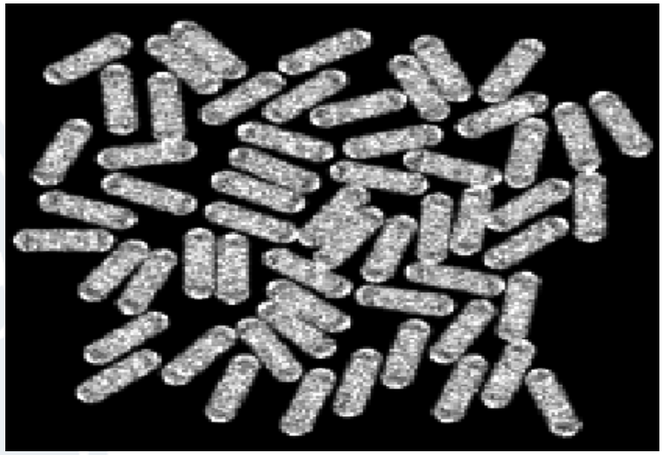

D. Convolve with Gaussian kernels

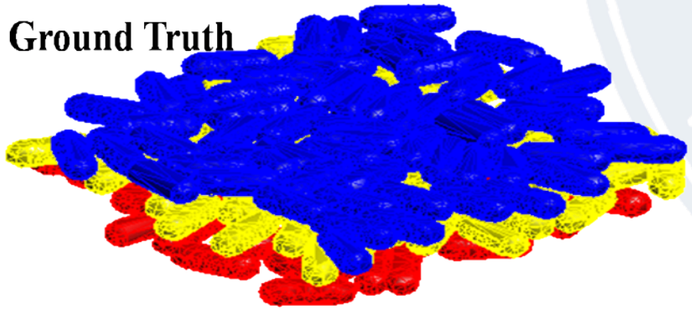

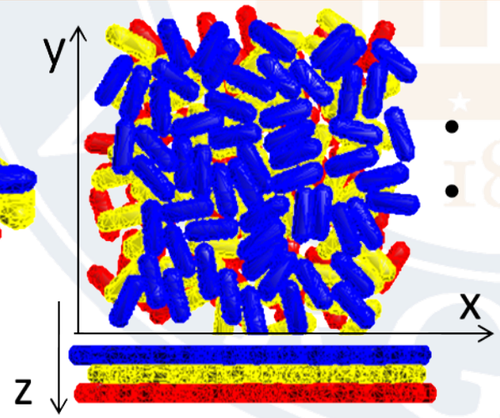

- Three layers
- Densely distributed

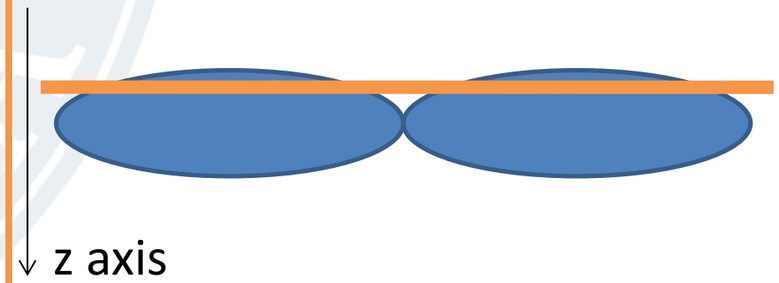

• Curvature-based seed selection

- Evaluating the Hessian of the image:

$$H = \begin{bmatrix} Ixx & Ixy \\ Iyx & Iyy \end{bmatrix}$$

- Select the most negative eigenvalues with highest curvature

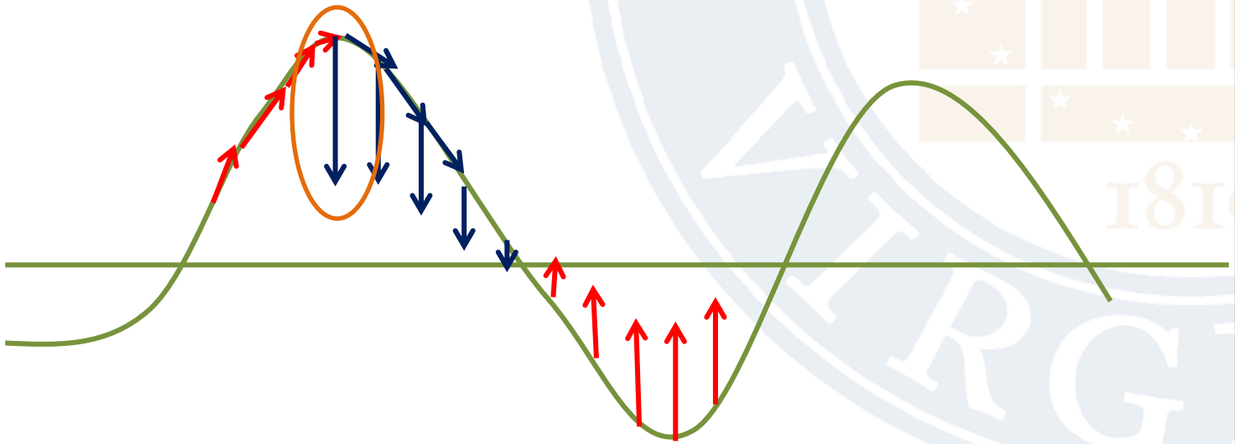

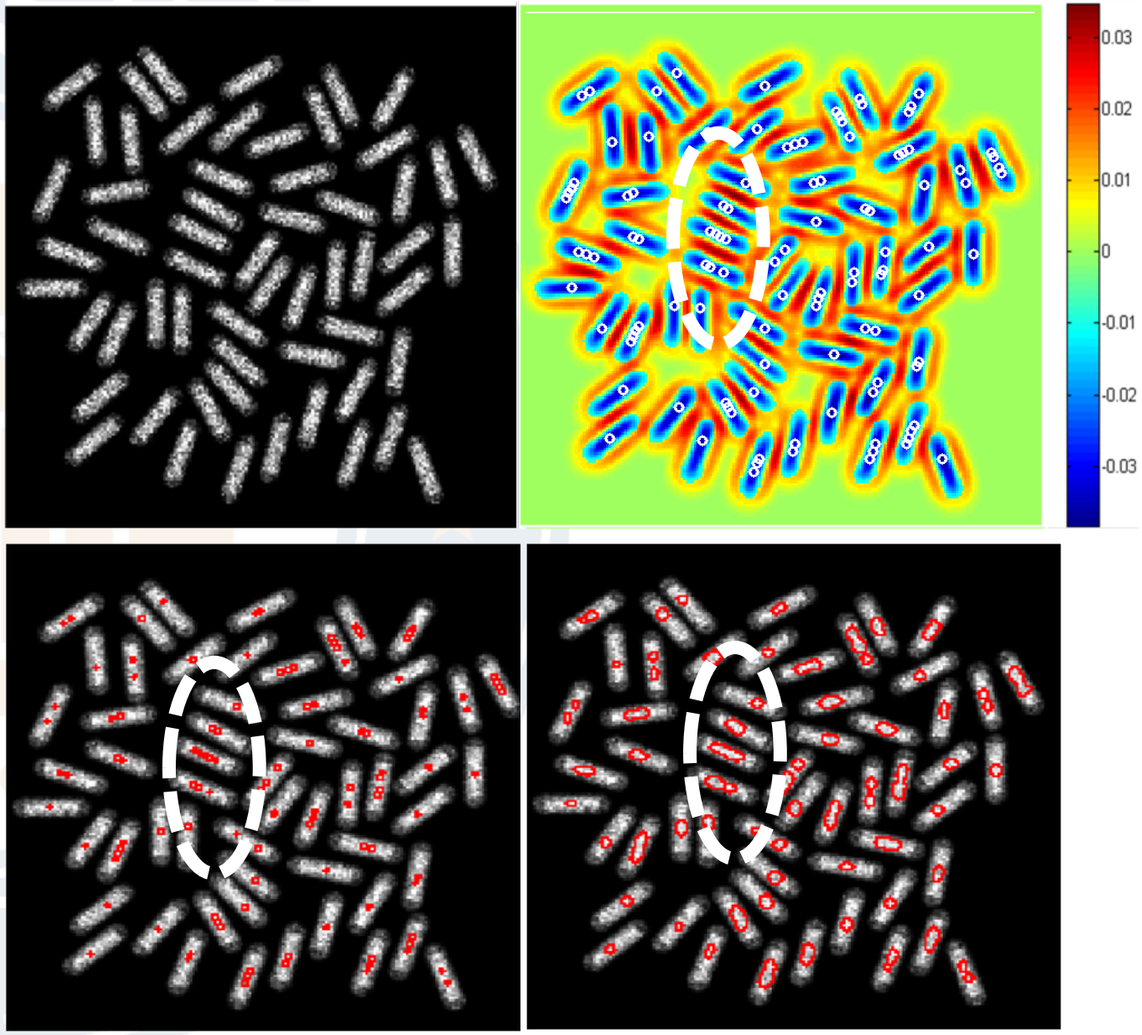

- # Iterative level set evolution

$$C = \{(x, y; t) : \phi(x, y; t) = 0\}$$

$$C_t = V\mathbf{N} \longrightarrow \phi_t = -V \mid \nabla\phi \mid$$

$$V = \begin{cases} 0 & , \quad \text{if SC} = 1 \\ g \cdot [1 - \varepsilon\kappa] - \beta\nabla g \cdot \mathbf{N}, & \text{otherwise} \end{cases}$$

Local affinity → **Control speed**

Smoothing

Slow down

Curvature term

$$\kappa = \operatorname{div}\left(\nabla\phi / |\nabla\phi|\right)$$

→ **Be smooth**

Outward normal force:

$$N = \nabla\phi / |\nabla\phi|$$

Edge indicator → **Move to edge**

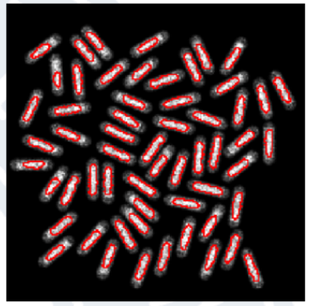

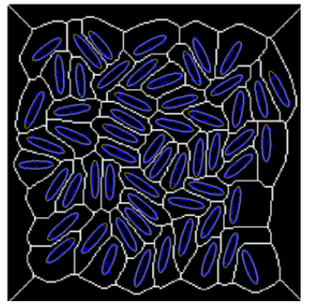

Local affinity [1]: based on the gray-scale intensity gradient

$$g(x, y) = e^{-E(x,y)/v}, E(x, y) = \frac{|\nabla I|}{G * |\nabla I| + \gamma}$$

High value in areas with low gradients

Contrast normalization

v: determines the magnitude of g

γ: constant, ensure E remain limited in some small gradients

[1] A. Levinshtein, A. Stere, K. N. Kutulakos, D. J. Fleet, S. J. Dickinson, and K. Siddiqi, "Turbopixels: Fast superpixels using geometric flows," IEEE Transactions on Pattern Analysis and Machine Intelligence, vol. 31, no. 12, pp. 2290–2297, 2009.

[2] Velocity representation refer to: C.O. Solorzano, R. Malladi, S.A. Lelievre, and S.J. Lockett, "Segmentation of nuclei and cells using membrane related protein markers," Journal of Microscopy, vol. 201, pp. 404–415, 2001.

- **Localization of individual bacteria**

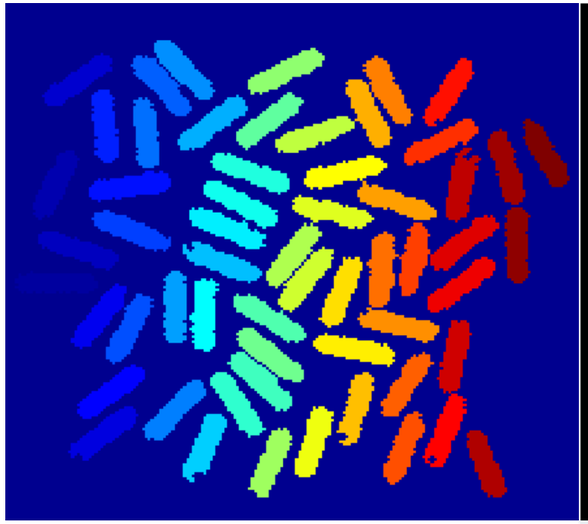
a. Preliminary contour

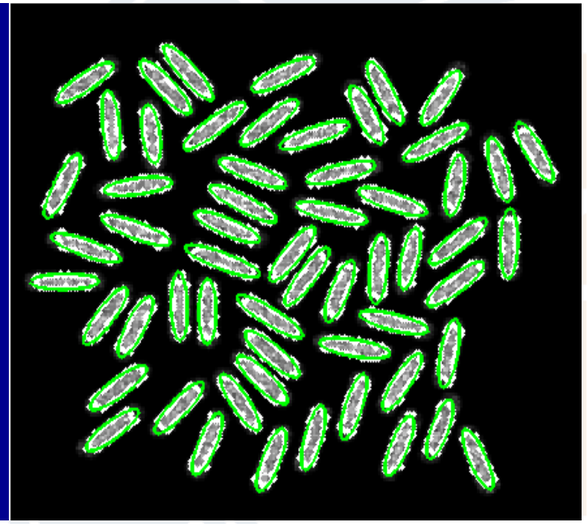
b. Ellipse fitting

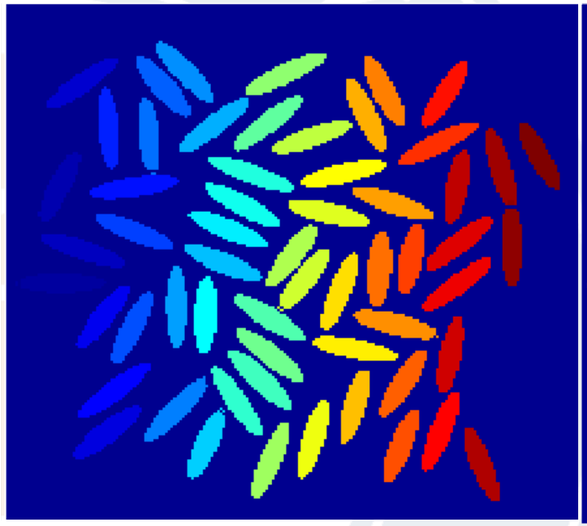
c. Localization

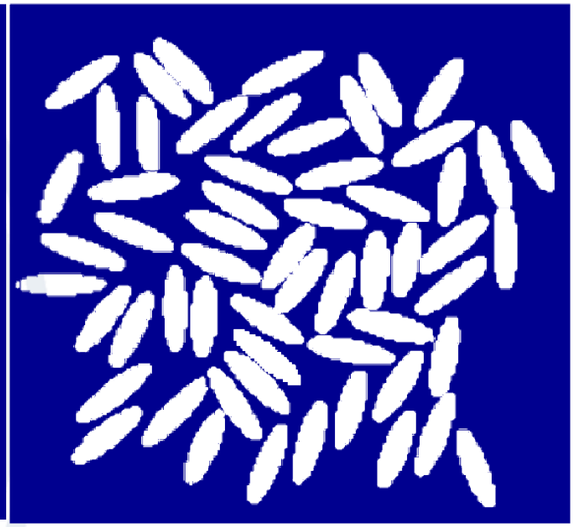
d. Smoothed background

Least square fitting by evaluating the conic form of the ellipse:

$$ax^2 + bxy + cy^2 + dx + ey + f = 0$$

- A. W. Fitzgibbon, M. Pilu, and R. B. Fisher, “Direct least squares fitting of ellipses,” 1996.

- **Stopping criterion**

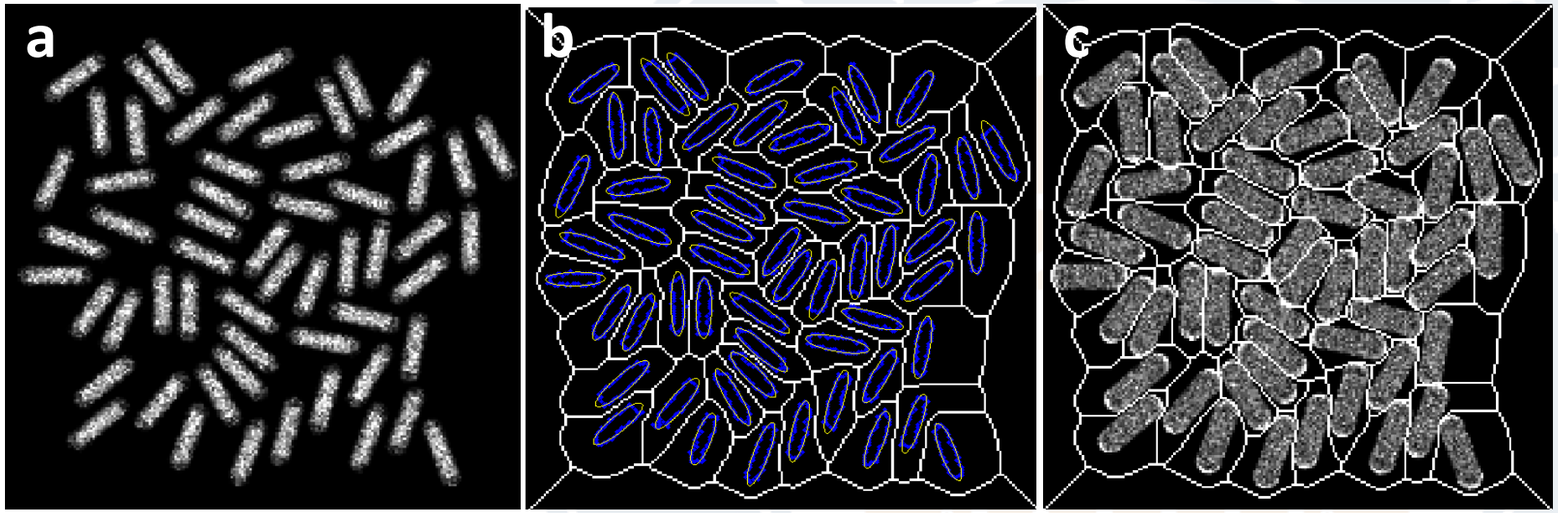

a: Original image;

b: Stopping criterion is set as the skeleton of *background* that excludes *ellipses*;

c: Stopping criterion is efficient for most situations;

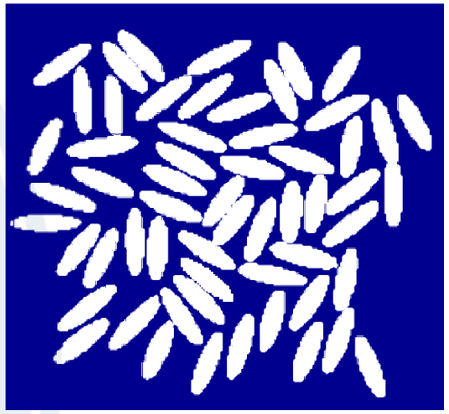

0 1 1 1 0 → 0 0 1 0 0
1 1 1 1 1 → 0 0 1 0 0
1 1 1 1 1 → 1 1 1 1 1
1 1 1 1 1 → 0 0 1 0 0
0 1 1 1 0 → 0 0 1 0 0

• Layer detection and re-initialization

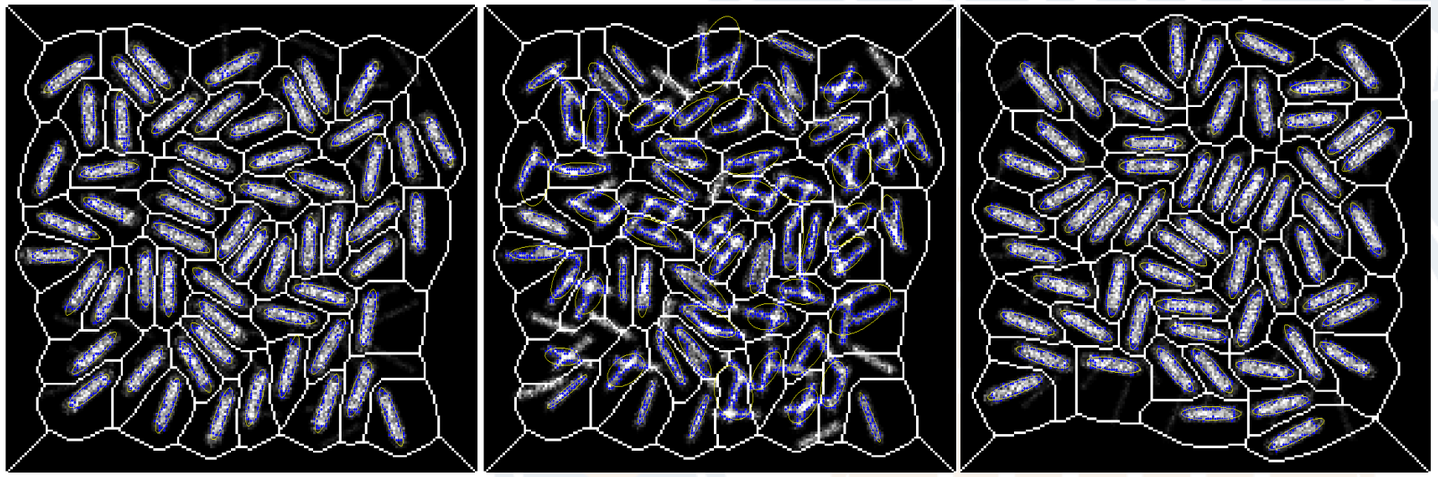

- Stopping criterion is re-initialized, when there is a layer change detected.

Automated Layer Detection

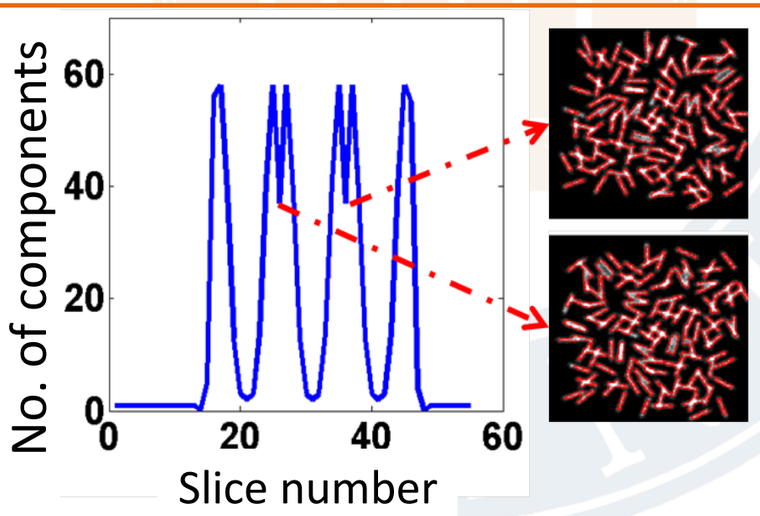

- Layers are automatically detected by identifying *sharp* local minima.

Experimental results

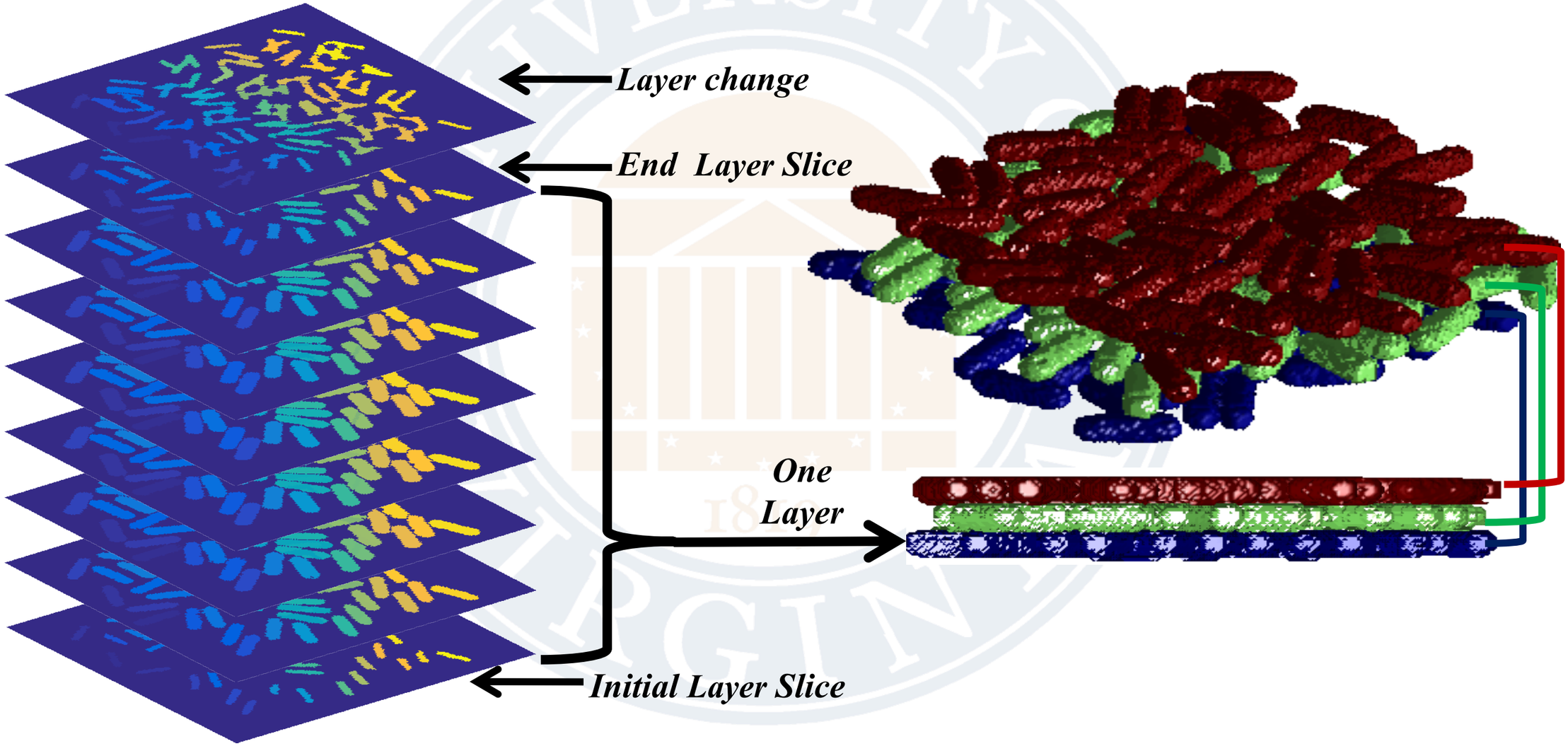

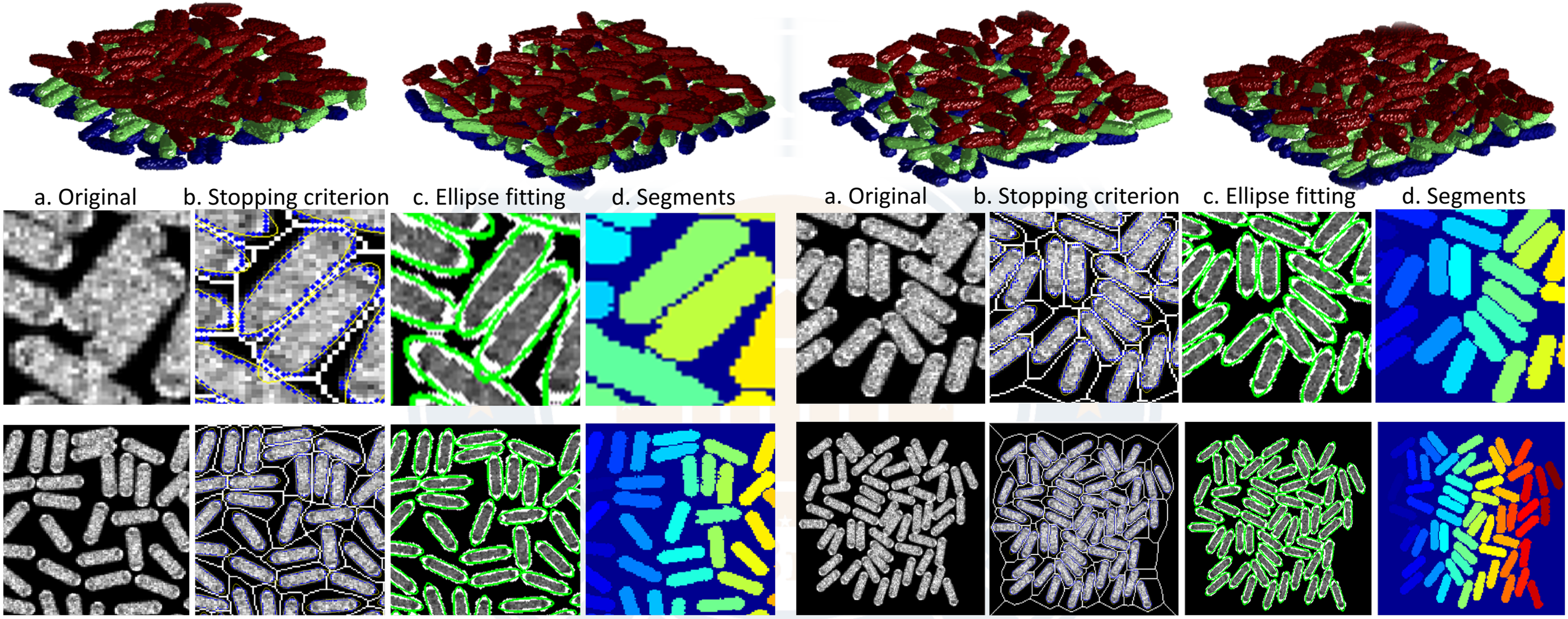

- **Locality**: the contours are always limited to a single-cell region;
- **Trackability**: locations and orientations are available for each individual bacterium.

- **Comparison of segmentation performance**

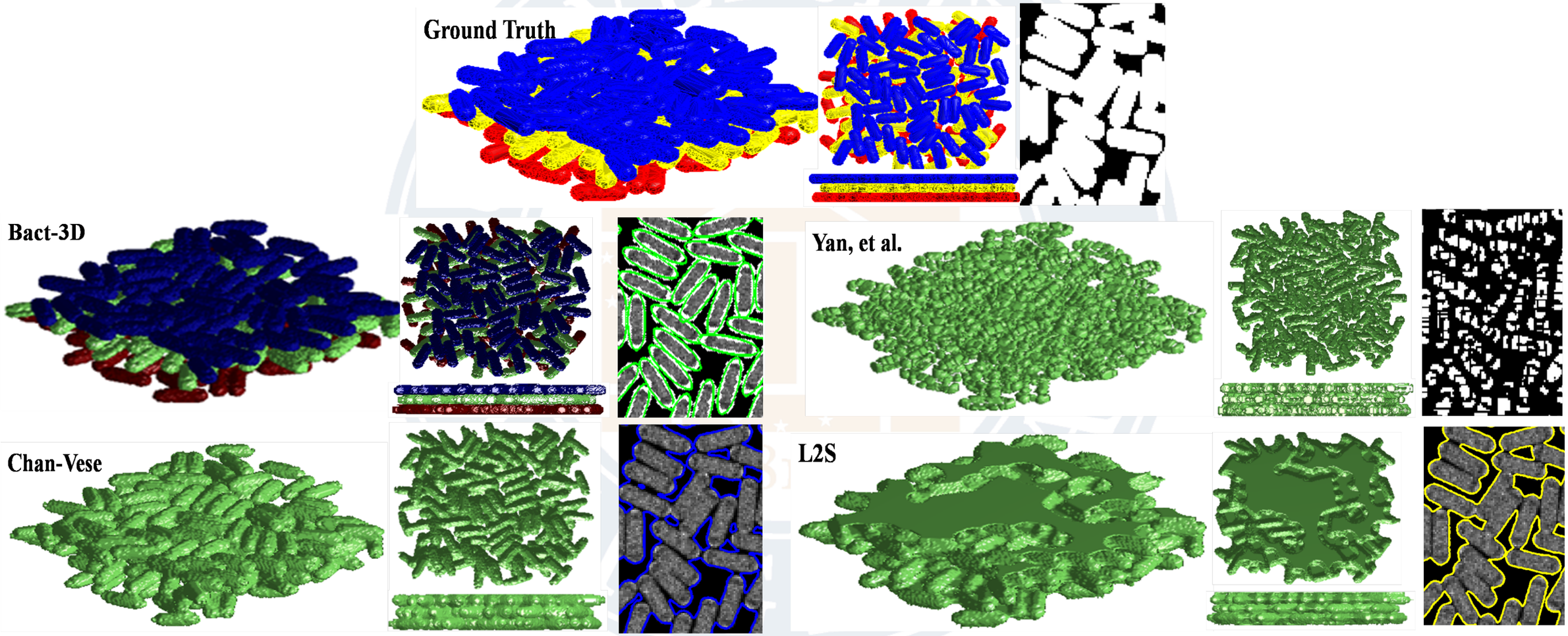

Dice Coefficient

- Compares similarities

$$Dice = \frac{2\left|V_g \cap V_t\right|}{\left|V_g\right| + \left|V_t\right|}$$

Mean squared error

- Compares averaged error

$$MSE = \frac{1}{Z} \cdot \left\|V_g - V_t\right\|_2^2$$

Cell detection accuracy

- Number of cells detected

$$CD = \frac{2\min(N_g, N_t)}{N_g + N_t}$$

Resolution 1	Dice	MSE	CD%
Bact-3D	0.871	0.084	**99.8**
Yan, et al.	0.558	0.240	56.54
Chan-Vese	**0.895**	**0.073**	5.41
L2S	0.891	0.075	5.27

Resolution 2	Dice	MSE	CD%
Bact-3D	0.861	0.089	**99.8**
Yan, et al.	0.546	0.245	72.2
Chan-Vese	0.834	0.105	15.7
L2S	**0.876**	**0.087**	4.52

Why are Bact-3D’s Dice and MSE not better than the other two?

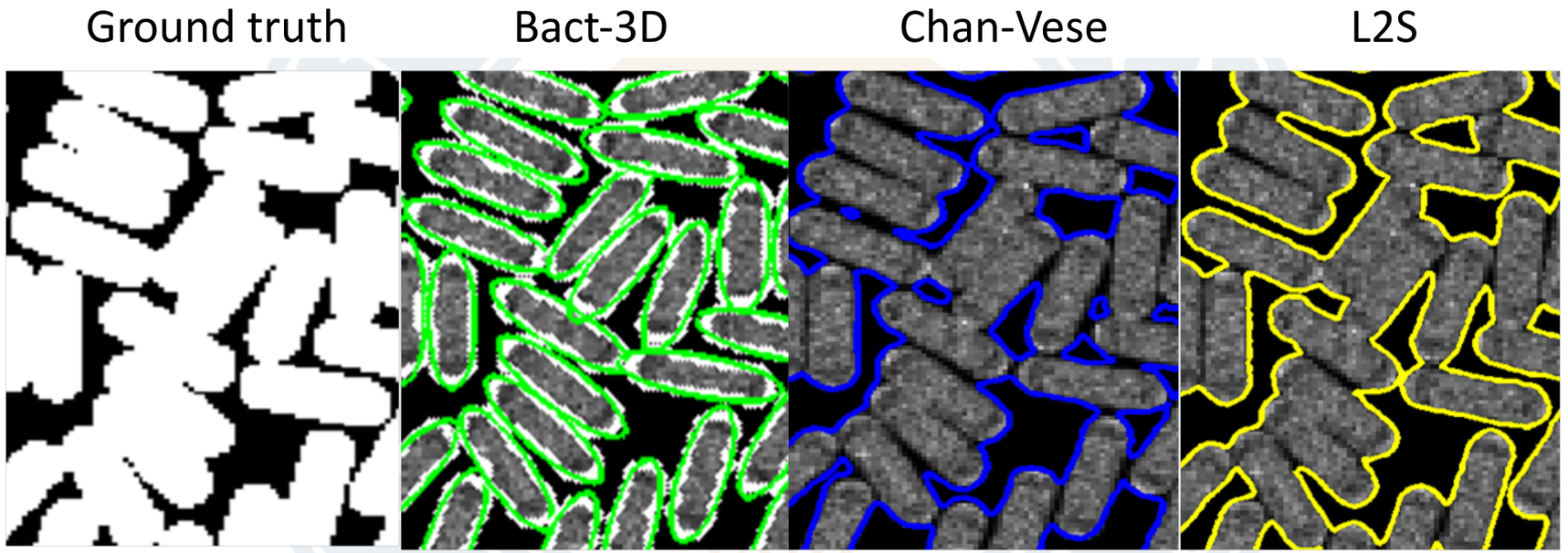

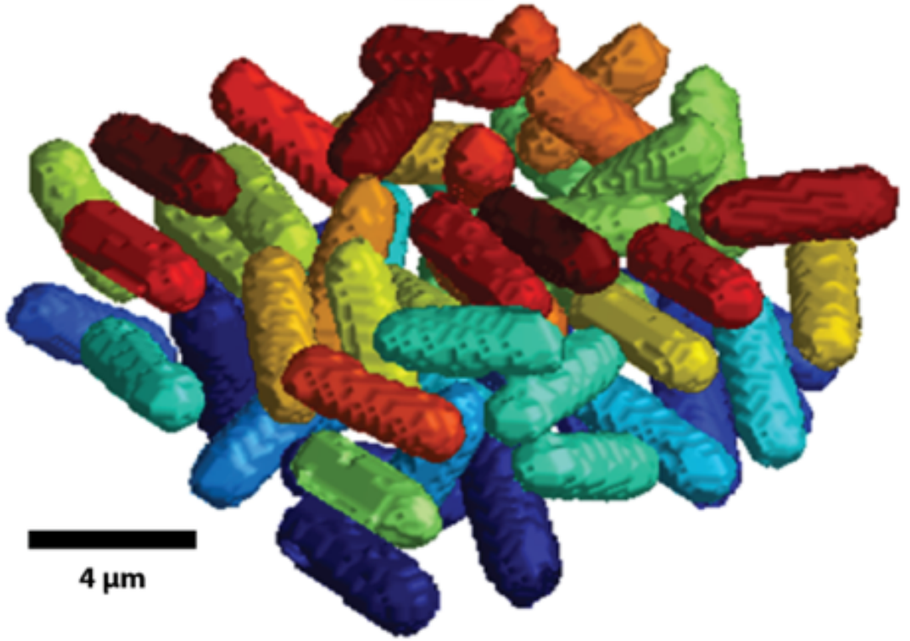

- New: no layer assumption
- Use Chan-Vese initialization to estimate orientation of cell; take 2D skeletons to make stopping criterion in X, Y, Z (via union of slices)
- Velocity of level set now depends on the distance to nearest stopping criterion (slow down near the stopping criterion)

From active contour to active surface: Bact-3Ds

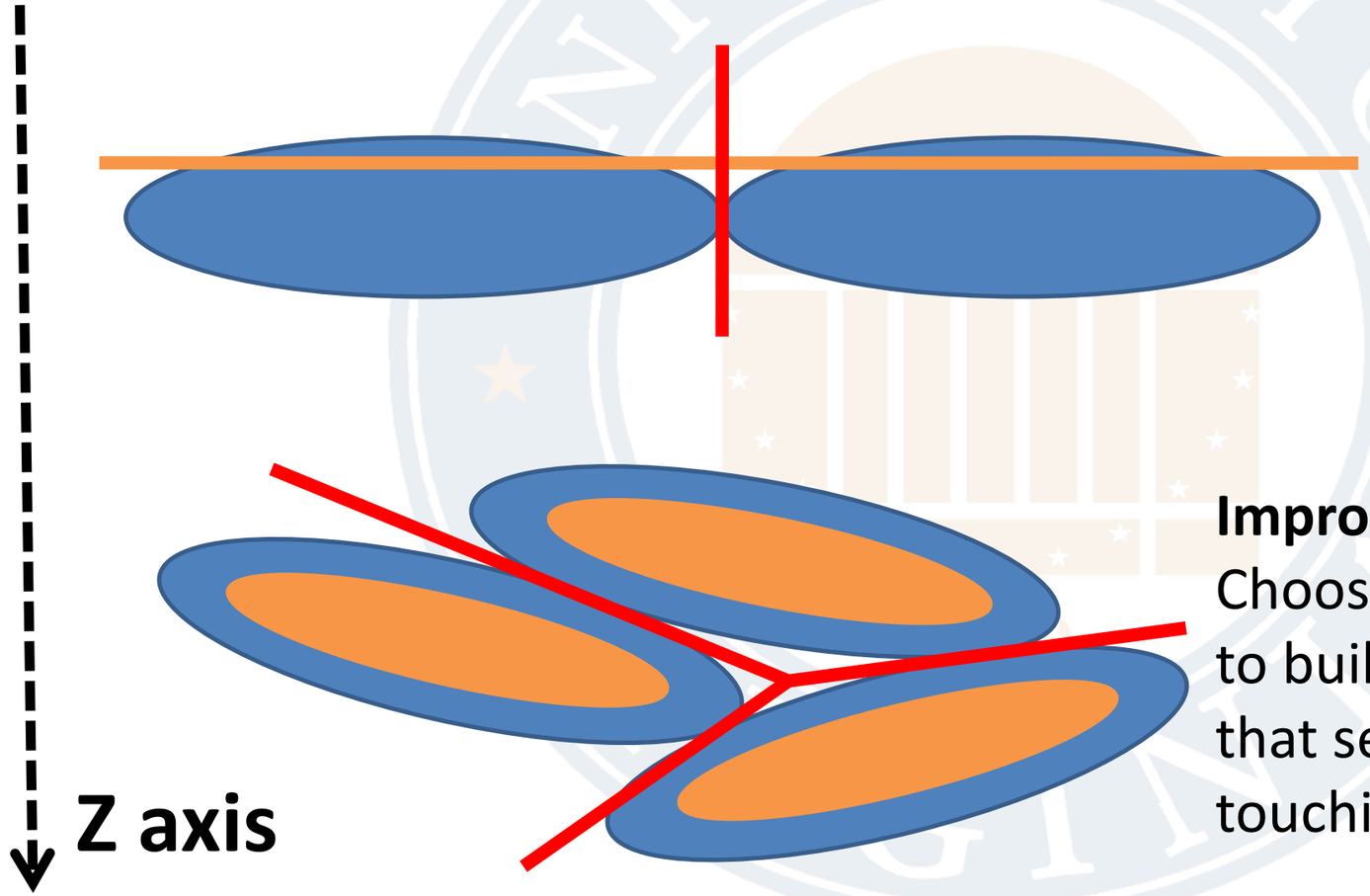

Old Method:
Choose orange slice
to build a **"red wall"**
that separates the
touching cells

Improved Method:
Choose orange layers inside
to build **"red walls"**
that separate the
touching cells

1. Seed Selection: 3D ChanVese

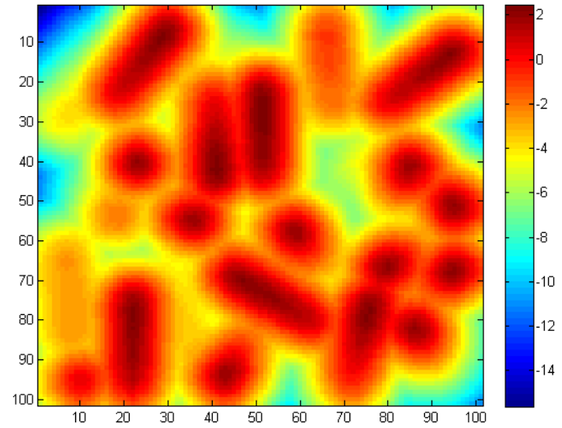

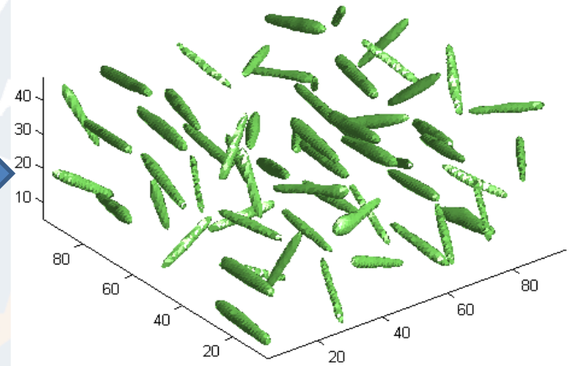

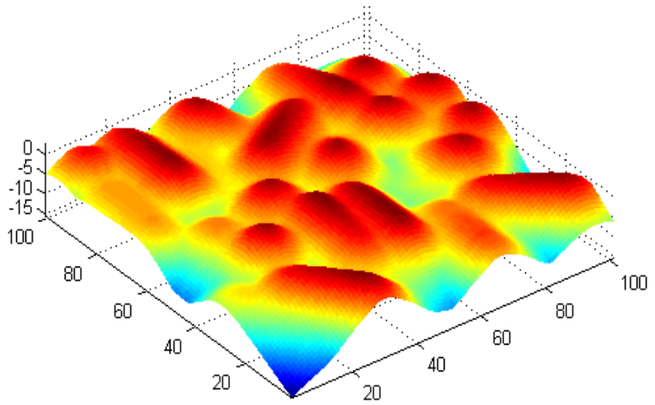

$$\phi(x, y, z; t)$$

2. Curvature-based active surface

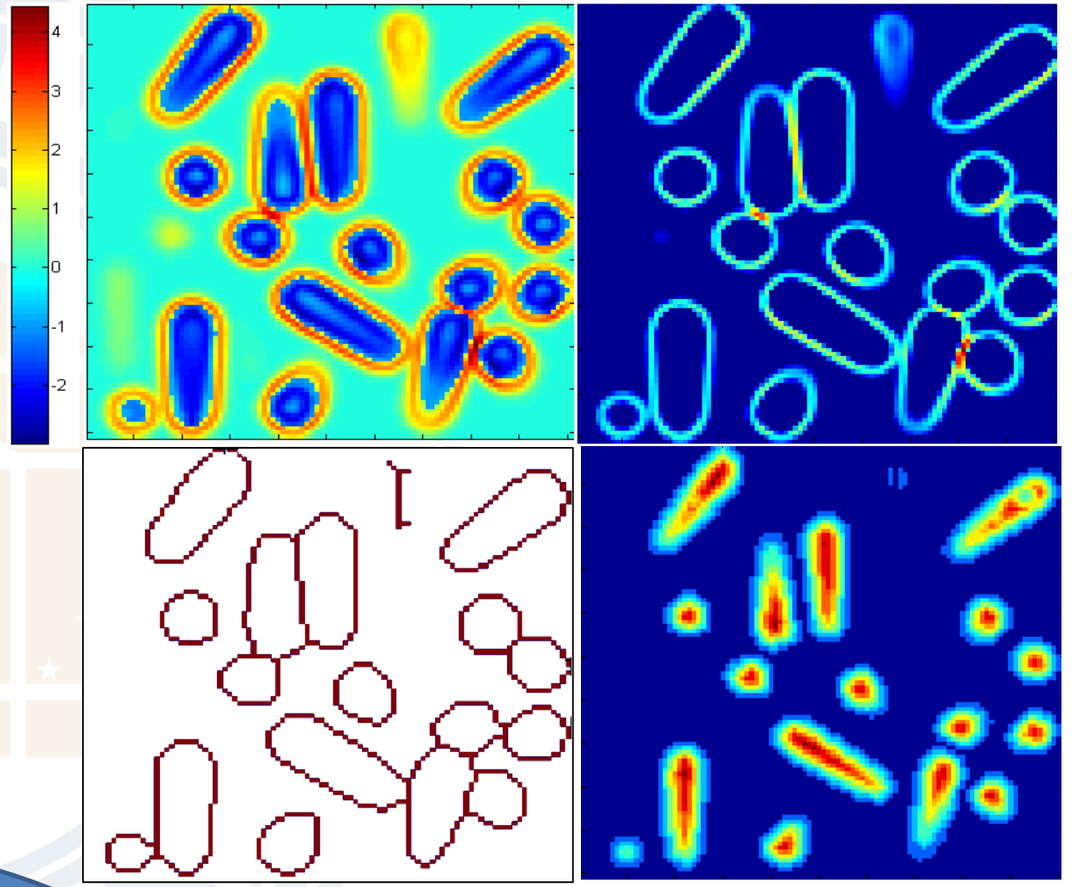

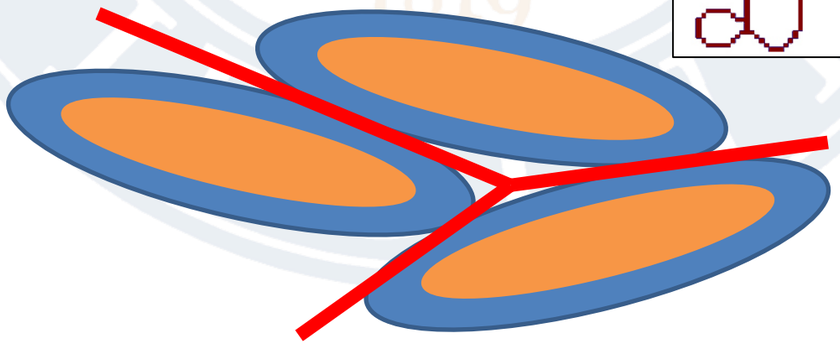

DVF: distance velocity field in geometric active surface

Sliced comparisons

3D viewers (detected No./ total No.)

Bact-3Ds

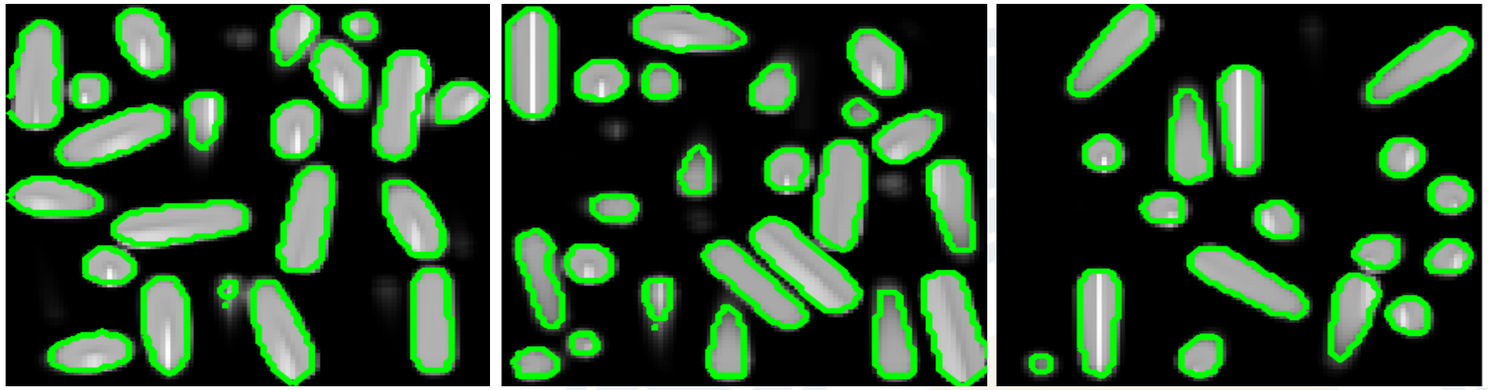

52/60

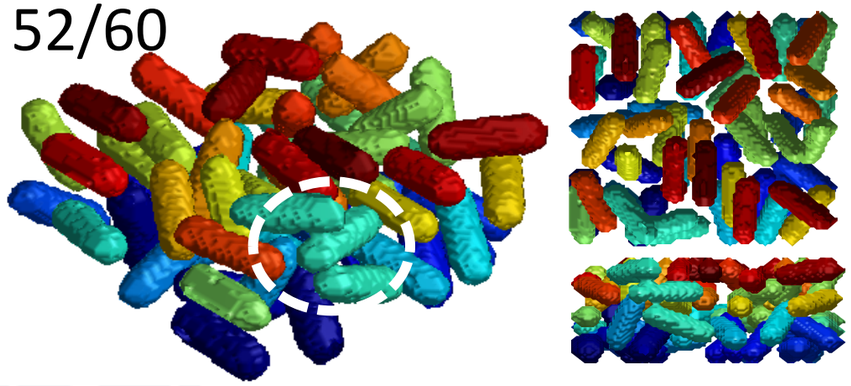

Bact-3D

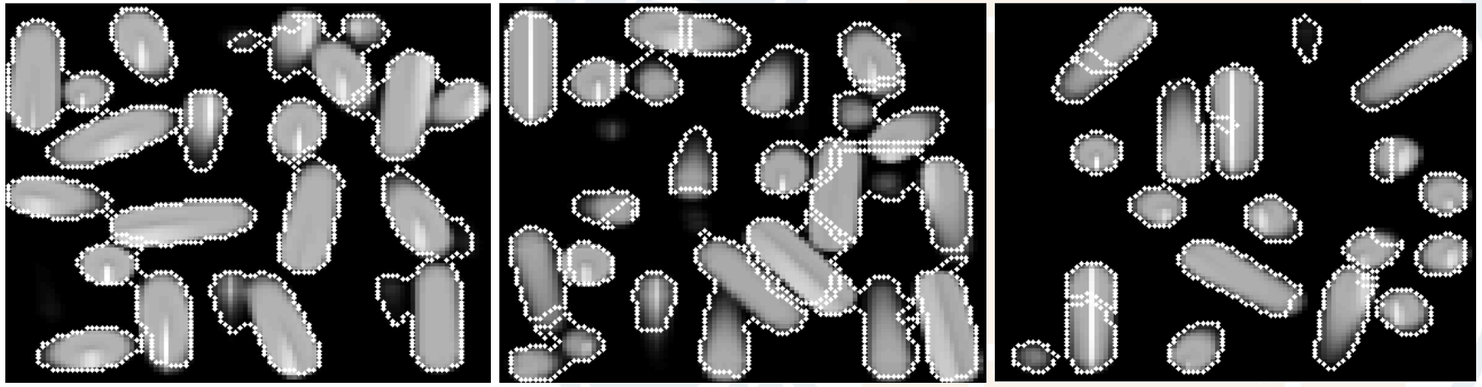

17/60

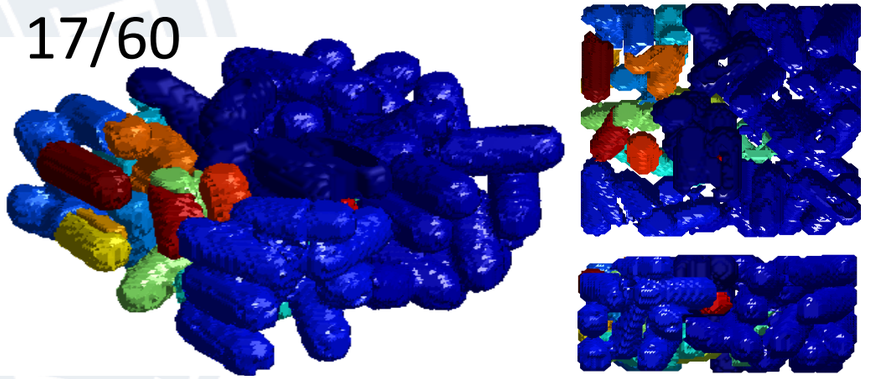

Chan-Vese

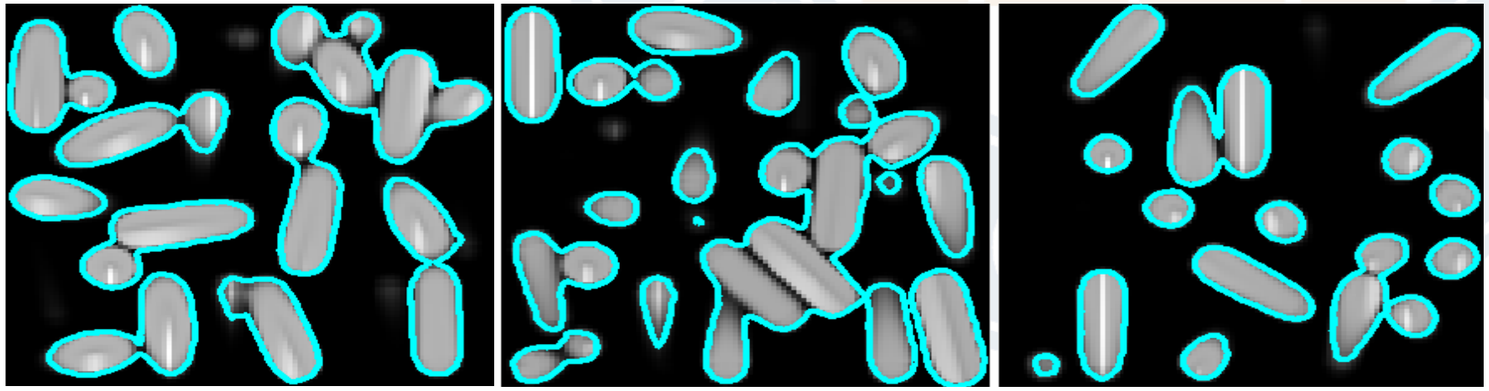

1/60

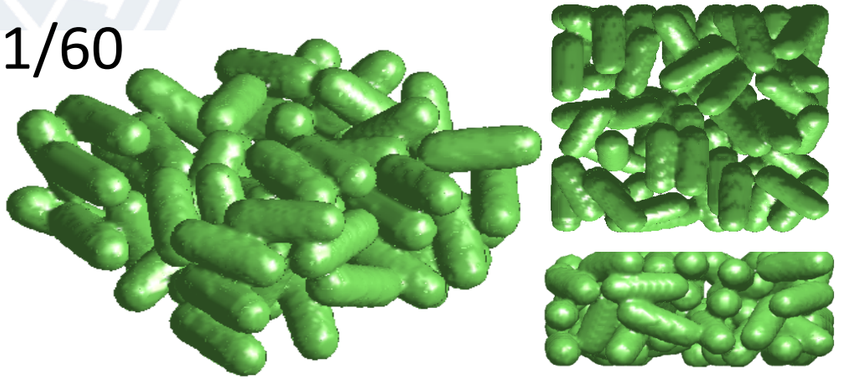

Conclusion

Super-resolution → Bact-3D

- Separate touching cells
- Reconstruct multilayered bacterial biofilms
- Provide tool for tracking cells and studying group structure

→ Modify to be robust for real data

How do cells communicate, share nutrients, discard waste and self-organize?

Andreas Gahlmann


Thank you!
谢谢！